Scripta Materialia 155 (2018) 68–72

Contents lists available at ScienceDirect

Scripta Materialia

journal homepage: www.elsevier.com/locate/scriptamat

Regular article

# Solute Sn-induced formation of composite $\beta'/\beta''$ precipitates in Al-Mg-Si alloy

Chunhui Liu [a,b,c], Peipei Ma [c], Lihua Zhan [a,b,c], Minghui Huang [a,b,c], Jianjun Li [a,b,*]

[a] State Key Laboratory of High-Performance Complex Manufacturing, Central South University, Changsha 410083, China
[b] School of Mechanical and Electrical Engineering, Central South University, Changsha 410083, China
[c] Light Alloy Research Institute of Central South University, Changsha 410083, China

ARTICLE INFO

*Article history:*
Received 22 May 2018
Received in revised form 10 June 2018
Accepted 11 June 2018
Available online xxxx

*Keywords:*
Al-Mg-Si alloys
Precipitation
Microalloying
Ageing
Scanning transmission electron microscopy

ABSTRACT

The composite $\beta'/\beta''$ precipitates rather than well-defined $\beta'$ phase form in trace-Sn containing Al-Mg-Si alloy peak-aged at 250 °C, leading to considerable morphological refinement. The preferential occupation of 2~6 adjacent Si sites of the tiny $\beta'$ phase by Sn and typical $\beta''$ substructure units covering the precipitates are frequently observed. The substructures grow upon further ageing into differently oriented $\beta''$ with 2~3 complete structural unit cells. It is inferred that the $\beta'$ ($Mg_9Si_{5-x}Sn_x$) forms initially on the Sn/vacancy complexes and then acts as heterogeneous nucleus for $\beta''$. These findings demonstrate Sn could fundamentally alter the pre−/precipitation behaviors in Al-Mg-Si alloys.



Al-Mg-Si alloys (6xxx series) constitute the most widely used Al alloys, and the last decade has seen ever increasing consumption of them in the transportation industry due to their good formability, light weight and low cost [1]. Extensive investigations have been conducted to elucidate the underlying mechanisms of age hardening behavior under various tempers [2–16]. The generally accepted precipitation sequence for this alloy system is as follows: SSSS (super-saturated solid solution) → atomic clusters/GPzones → $\beta''$ → $\beta'$, while U1, U2 and B′ can also form in alloy with low Mg/Si ratio [3, 8, 11]. The $\beta''$ phase ($Mg_5Si_6$) with a monoclinic crystal structure (space group: C2/m, lattice parameters: a = 1.516 nm, b = 0.405 nm, c = 0.674 nm, β = 105.3°) [14–16] is normally regarded as more effective in strengthening than the $\beta'$ phase ($Mg_9Si_5$) with a hexagonal crystal structure (space group: $P6_3/m$, lattice parameters: a = 0.715 nm, c = 1.215 nm, γ = 120°) [12]. During manufacturing process, natural pre-ageing would occur before artificial ageing [5, 7]. In addition, the hardening potential at high artificial ageing temperature is relatively low [17, 18]. These two phenomena are common to all heat treatable Al alloys but can exert very negative effects on the ageing kinetics and achievable maximum hardness of Al-Mg-Si alloys. The studies to alleviate these adverse effects have attracted a lot of interests [5, 7, 9, 18–21]. The main strategies are physical metallurgical methods such as interrupted quenching [20] and novel design of composition [22]. Microalloying Sn stands out for its versatile roles in controlling the precipitation process [7, 13, 18]. Sn tends to bind strongly with vacancies at room temperature while weakly at elevated artificial ageing temperature (~180 °C), leading to "diffusion on demand" of solutes which can be used to suppress natural ageing without deteriorating artificial ageing [7, 19]. The expedited age hardening and much higher peak hardness occurring in the Sn-added Al-Mg-Si alloy aged at 210–250 °C [18] demonstrates Sn could also considerably influence the diffusion and precipitation at high temperatures. Though theoretical modeling was conducted to explain these phenomena [18, 19], it remains a puzzle for the precise role played by Sn during the precipitation process due to the lack of direct experimental evidence.

In the present work, the precipitates in the Sn-added Al-Mg-Si alloy peak-aged at 250 °C have been observed in detail by atomic-scale high-angle annular dark-field scanning transmission electron microscopy (HAADF-STEM) and high-resolution chemical mapping. The $\beta'$ with the Si atom columns partially substituted by Sn forms firstly. The $\beta''$ then grows on $\beta'$, leading to the formation of $\beta''/\beta'$ composite precipitate. More importantly, our results provide mechanistic insights into the trace-Sn enhanced precipitation hardening in Al-Mg-Si alloys.

The alloy with composition of Al-0.93 Mg-0.58Si-0.08Sn-0.2Fe-0.12Mn (wt%) was used in this study. Another alloy free of Sn but possessing the same composition was prepared as control. Small pieces of samples were firstly solution treated in an air circulating furnace at 575 °C for 20 min and then water quenched to room temperature. Immediately after then, the samples were artificially aged in an oil bath at 250 °C. According to previous investigations [5, 18], the samples were aged for 5 and 10 min, respectively. The TEM specimens were

* Corresponding author at: State Key Laboratory of High-Performance Complex Manufacturing, Central South University, Changsha 410083, China.
*E-mail addresses:* chunhuiliu@csu.edu.cn, (C. Liu), mejjli@csu.edu.cn (J. Li).

https://doi.org/10.1016/j.scriptamat.2018.06.028
1359-6462/

prepared by mechanical thinning and then by standard twin-jet electropolishing in a methanol solution mixed with 25% nitric acid below −30 °C. TEM characterization were performed with the electron beam parallel to the $\langle 001\rangle_{Al}$ directions on a FEI Tecnai F20 operated at 200 kV. HAADF-STEM imaging and elemental mapping were carried out by using a Cs-corrected FEI Titan operated at 300 kV and equipped with high-performance X-ray energy dispersive spectroscopy (EDS) detectors. The raw HAADF-STEM images were Fast Fourier transform (FFT) filtered to remove the high-frequency noises. No additional image processing was performed. The first principle calculations were conducted using Vienna ab initio Simulation Package (VASP) based on the density functional theory (DFT). The generalized gradient approximation (GGA) and ultrasoft pseudopotentials were adopted [23, 24]. Full relaxations including volume and ionic positions were performed with a plane-wave energy cut-off of 350 eV. The formation energy of the proposed precipitate structure with respect to the solid solution was defined and calculated using a well-developed method, with the details can be found elsewhere [11, 25].

The precipitates in Al-Mg-Si alloys are generally needle-like or rod-like and grow along three equivalent $\langle 001\rangle_{Al}$ zone axes [3, 5]. As shown in Fig. 1a (sample peak-aged for 5 min), the precipitates in the Sn-added alloy exhibit a very fine and uniform distribution with an average length of about 20–30 nm. The cross-sections of the edge-on precipitates appear as dark dots and were examined carefully at high magnifications. One representative high-resolution TEM (HRTEM) image is displayed in Fig. 1b, but is poorly determined. It is very difficult to identify the lattice structure of the seemingly disordered precipitate. In stark contrast, the Sn-free counterpart feature coarse and very long precipitates (>300 nm in length) oriented along the $\langle 001\rangle_{Al}$ directions (see Fig. 1c), and this finding is consistent with previous observations [5]. The Sn-induced significant morphological change observed in this study should be responsible for the ultrafast age hardening in Sn-added Al-Mg-Si alloy [18]. Lattice parameters measurements through HRTEM images show the precipitates in Sn-free alloy possess a crystal structure the same with $\beta'$ phase (Fig. 1d). The difference in the precipitate crystal structures in the alloys with and without Sn indicates Sn may also affect the precipitation pathway during the decomposition process.

HAADF-STEM imaging can provide *Z*-contrast (*Z* is atomic number) and was then employed to image the precipitates in greater details for the peak-aged Sn-added samples. Before analyzing the images, we firstly recall the structural features of both $\beta''$ and $\beta'$ phases. Fig. 2a shows schematically the atomic structure models of $\beta''$ and $\beta'$ phase viewed along different crystallographic orientations [3, 6, 12]. One unique substructure of $\beta''$ phase is the low-density cylinder (LDC) composed of Mg atom columns [11]. The LDC generates an "eye-like" feature in the S/TEM images [3, 6]. The triangular substructure unit with the Si atom column located at the center and surrounded by Mg atom columns is typical of $\beta'$ phase [12]. These characteristic substructures will be used to discern $\beta''$ and $\beta'$ phase. As shown in Fig. 2b, most of the cross-sections of the precipitates are decorated with a bright dot at the center in the low-magnification HAADF-STEM image. This suggests there are Sn-enrichments inside the fine precipitates because only Sn with a much higher atomic number than the other atom species can generate such a bright contrast. Four representative atomic-scale HAADF-STEM images are shown in Fig. 2c–f, respectively. The arresting feature is the bright atom columns in close proximity to each other. The bright columns have a number ranging from 2 to 6 and are arranged in a

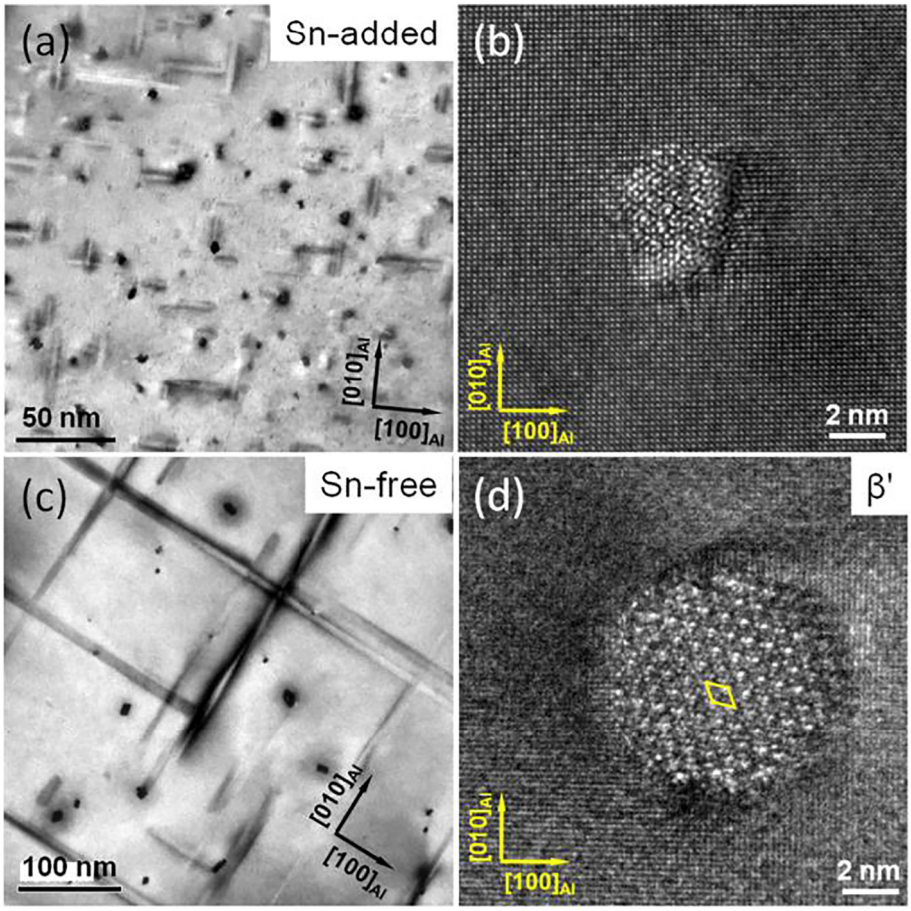


**Fig. 1.** TEM images of the precipitates in Al-Mg-Si alloy aged at 250 °C for 5 min: (a) Low magnification bright-field images and (b) representative HRTEM images for Sn-added alloy; (c) Low magnification bright-field images and (d) representative HRTEM images for Sn-free alloy.